Applied Physics Letters

Nonvolatile memory based on redox-active ruthenium molecular monolayers

Cite as: Appl. Phys. Lett. **115**, 162102 (2019); https://doi.org/10.1063/1.5108675
Submitted: 30 April 2019 . Accepted: 02 October 2019 . Published Online: 14 October 2019

Kai Jiang, Sujitra J. Pookpanratana, Tong Ren, Sean N. Natoli, Brent A. Sperling, Joseph Robertson, Curt A. Richter, Sheng Yu, and Qiliang Li

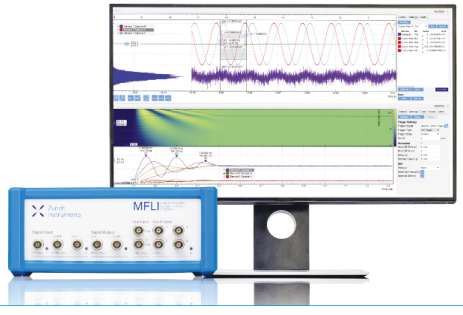

Applied Physics Letters ARTICLE scitation.org/journal/apl

Nonvolatile memory based on redox-active ruthenium molecular monolayers

Cite as: Appl. Phys. Lett. **115**, 162102 (2019); doi: 10.1063/1.5108675
Submitted: 30 April 2019 · Accepted: 2 October 2019 ·
Published Online: 14 October 2019

Kai Jiang,[1,2] Sujitra J. Pookpanratana,[2] Tong Ren,[3] Sean N. Natoli,[3] Brent A. Sperling,[4] Joseph Robertson,[5] Curt A. Richter,[2] Sheng Yu,[1] and Qiliang Li[1,2,a)]

AFFILIATIONS

[1]Department of Electrical and Computer Engineering, George Mason University, Fairfax, Virginia 22030, USA
[2]Nanoscale Device Characterization Division, National Institute of Standards and Technology (NIST), Gaithersburg, Maryland 20899, USA
[3]Department of Chemistry, Purdue University, West Lafayette, Indiana 47907, USA
[4]Chemical Sciences Division, NIST, Gaithersburg, Maryland 20899, USA
[5]Microsystems and Nanotechnology Division, NIST, Gaithersburg, Maryland 20899, USA

[a)]**Author to whom correspondence should be addressed:** qli6@gmu.edu

ABSTRACT

A monolayer of diruthenium molecules was self-assembled onto the silicon oxide surface in a semiconductor capacitor structure with a "click" reaction for nonvolatile memory applications. The attachment of the active molecular monolayer was verified by x-ray photoelectron spectroscopy. The prototypical capacitor memory devices in this work employed a metal/oxide/molecule/oxide/Si structure. With the intrinsic redox-active charge-storage properties of diruthenium molecules, these capacitor memory devices exhibited fast Program and Erase speed, excellent endurance performance with negligible degradation of the memory window after 10^5 program/erase cycles, and very good 10-year memory retention. These experimental results indicate that the redox-active ruthenium molecular memory is very promising for use in nonvolatile memory applications.

Over the past decade, semiconductor memory technology has been one of the major driving forces in developing portable devices, such as smart phones, tablets, and wearable electronics. The market demand for high-performance, high-density nonvolatile memory (NVM) increases exponentially. However, conventional flash memory based on polysilicon or Si_3N_4 charge storage layers is facing fundamental and physical limits arising from further dimensional scaling to enable increasing memory density. A tremendous effort to develop emerging memory materials with excellent electrical and physical properties has been made in both academia and industry.

Memory devices based on organic materials represent one of the emerging technologies[1] for information storage to improve memory performance and satisfy the exponential demand for high-density nonvolatile memory for low-power portable devices. In comparison with traditional flash memory devices, molecular flash memory can be fabricated at lower cost and operated with low-power consumption.[2] A variety of memory devices based on organic molecules have shown with remarkable memory effects,[3–5] and organic molecular memory devices on different mechanisms have been reported in recent years. The reported emerging molecule-containing memory devices included floating-gate memory,[6–13] resistive switching memory,[14–16] chargeable electret memory,[17–19] and ferroelectric memory.[20,21] Among them, memory devices based on redox-active molecules have attracted great interest due to their inherent and relatively stable redox processes for charge storage.[22] Substantial improvement in memory window, retention, endurance, and multibit storage capability has been achieved by applying organic molecular charge storage layers.[23,24]

In a redox-active molecular flash memory cell, the redox-active molecules have distinct oxidation and reduction states accessible at different applied voltages, enabling stable binary or multiple states for charge storage like that of traditional charge trapping materials.[25] Compared to polysilicon and Si_3N_4 charge storage layers, redox-active molecules have the advantage of intrinsic molecular scalability, multiple bits, and tunable electronic properties to achieve ultrahigh storage density.[26] In addition, redox molecules can be tuned to attach onto different kinds of semiconductor materials[27] and form self-assembled few-layer or monolayer structures with low-cost processes, usually a

solution-based process, which provides a great advantage for promising commercial memory applications in the future.

Recently, many studies on organic molecule-based charge trapping memory devices have been reported. Lee *et al.* reported a strong memory behavior induced by n-type doping of p-type conjugated polymers.[26] Tseng *et al.* reported a retention improvement by applying a double-floating gate which has both hole carrier trap units and electron carrier trap units, with the flexible pentacene molecule acting as the channel.[8] Although many kinds of molecular memory devices were reported, retention (information hold-time) is still a drawback as it is necessary to store the data for more than ten years.[5,28,29] In this work, we have fabricated memory cells with a metal-Al_2O_3-Ru_2-SiO_2-silicon (MAROS) structure and investigated their memory characteristics. A Si-molecular integration process to hold the redox-active diruthenium (Ru_2) molecules was applied, and the memory performance of MAROS capacitor structure was studied. A distinguished charge storage efficiency was exhibited with a 5.2 V memory window shown under a sweeping gate voltage of ±9 V. The degradation anticipation estimated by the measured data indicated that 72% of the initial memory window will remain after 10 years. The response with even a ±10 V/10μs gate bias pulse demonstrated that our devices were competent for future fast writing/reading requirements.

To engineer the molecular memory, we selected a newly synthesized diruthenium-based molecule synthesized as the functional charge storage layer. Its chemical formula is $C_{50}H_{32}N_8Cl_{13}Ru_2$[30] (referred to as Ru_2) with a chemical structure shown in Fig. 1(c). This Ru_2 molecule represents a class of molecules which allow for tuning the highest occupied molecular orbital (HOMO) and lowest unoccupied molecular orbital (LUMO) levels by varying the axial ligands X and Y without interfering with the surface attachment by the click reaction. The synthesis methods of Ru_2 molecules with different X and Y ligands are quite similar. The tuning of redox-active Ru_2 molecules also provides a method for further memory performance improvement. In this work, X = hydrogen and Y = chlorine are picked, and the HOMO and LUMO levels are located at −5.83 eV and −4.48 eV,[30,32] respectively. All solvents for the chemical click attachment were purchased from Sigma-Aldrich and used without further purification.

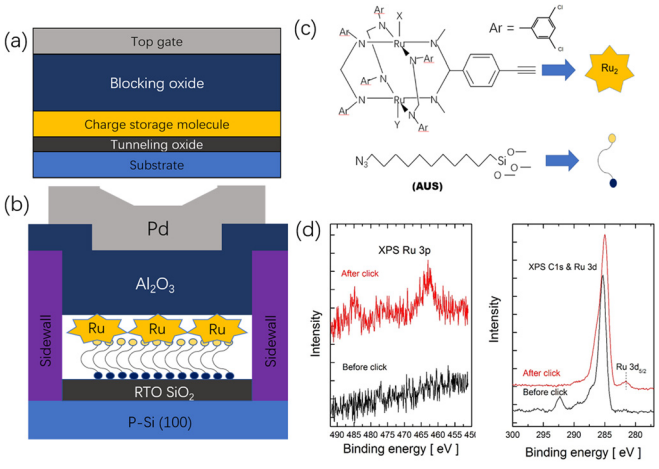

FIG. 1. Schematic cross section (not to scale) of a (a) prototype Flash-based memory device and (b) the MAROS capacitor structure used in this study. (c) The structure of the redox-active Ru_2 molecule and the aliphatic AUS are shown on the left, and the corresponding molecular cartoons are defined on the right. (d) XPS spectra of the molecular layer before and after attachment of Ru in the (left) Ru 3p region and (right) C 1s and Ru 3d regions. Before click: AUS/SiO_2/Si; after click: Ru+AUS/SiO_2/Si.

The metal-oxide-semiconductor (MOS) capacitor structure, applied in our flash-based memory devices [Fig. 1(a)], was fabricated and used for the attachment of the redox-active Ru_2 molecules as the charge trapping layer [Figs. 1(b) and 1(c)]. The fabrication process steps are described below. First, SiO_2 (≈290 nm) is thermally grown on an RCA-cleaned lightly p-doped Si (100) substrate followed by the definition of square active areas (≈100 μm wide) with photolithography and HF etching. Fabrication continues with the growth of ≈2 nm SiO_2 in the active areas by rapid thermal oxidation at 840 °C for 2 min. This thin high-quality SiO_2 acts as the tunneling oxide. The Ru_2 molecules are attached onto the device substrates by click chemistry with a linker molecule which has been reported by Pookpanratana *et al.*[31] Then, the Ru_2 molecular self-assembled monolayer (SAM) is covered immediately with ≈30 nm Al_2O_3 by the atomic layer deposition (ALD) method at 100 °C. Trimethyl-aluminium and H_2O are the precursors for the ALD process, and the thickness of Al_2O_3 is ascertained by the ellipsometry measurement. Finally, a Pd top gate (≈100 nm) is deposited and patterned on Al_2O_3 using an electron-beam evaporator.

X-ray photoelectron spectroscopy (XPS) measurements were performed by using a Kratos Axis Ultra instrument equipped with monochromatized Al Kα photons. The atomic force microscopy (AFM) images were obtained by using a Bruker Dimension FastScan. Electrical characteristics were measured in a dark environment with a commercial probe station. Bias was applied between the metal gate and the silicon substrate during all the electrical measurements. A series of capacitance-voltage measurements at various frequencies were applied by using an Agilent E4980A LCR meter. Pulse response sensitivity measurements were implemented with an Agilent 4156 Semiconductor Parameter Analyzer. A Hewlett Packard 33120A waveform generator was applied to measure the program/erase endurance.

Cyclic voltammetry (CV) measurements were performed with a Solartron potentiostat to verify the redox properties. The electrolyte was 0.1 mol/L tetrabutylammonium hexafluorophosphate in anhydrous acetonitrile and was deoxygenated with dry N_2 prior to use. A three-electrode cell configuration was used with the Ru_2 molecule clicked onto native oxide/Si as the working electrode (WE, area = 0.32 cm^2). The cell is completed with a platinum wire counter electrode and a silver quasireference (AgQRE) electrode. The sweep rate was 10 mV/s.

To confirm the chemical attachment of the molecules, AFM and XPS measurements were performed. The AFM images of a bare Si substrate (left), a Si substrate with an azidoundecyltrimethoxysilane (AUS) linkage molecule (middle), and a sample with Ru_2 SAM on the Si substrate (right) are shown in Fig. 2. The surface morphology investigated by AFM in semicontact mode revealed relatively smooth film surfaces and homogeneous monolayers. The root mean square (rms) roughness, R_{rms}, increased after the molecule attachment process. The R_{rms} of the bare substrate, AUS layer, and the final diruthenium layer for a 1 μm × 1 μm scan area were found to be ≈0.16 nm, 0.31 nm, and 0.64 nm, respectively. To directly confirm the chemical attachment information of the Ru_2 molecular SAM, Fig. 1(d) presents the

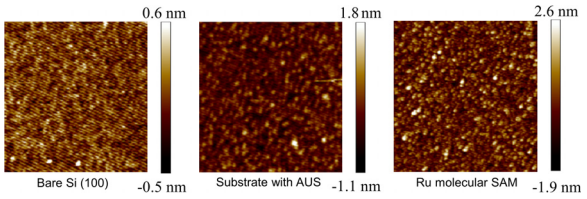

FIG. 2. AFM images of (left) bare Si (100), (center) substrate with AUS, and (right) Ru molecular SAM on the substrate.

XPS spectra gathered from the Ru_2-containing sample ("after click") and the AUS linker ("before click"). Ru $3d_{5/2}$ and Ru 3p peaks can be detected in the spectra of the Ru_2 SAM in contrast to the AUS linker surface, indicating that the Ru_2 molecule has been attached on the SiO_2 surface. The coverage density of Ru_2 molecules on the SiO_2/Si substrate is estimated as 0.3 molecules per nm^2 by the calculation of the Ru 3d and Si 2p XPS spectral lines with the Si substrate as the reference.

The CV measurements of the attached Ru_2 molecules on SiO_2/Si substrates (as the WE) are shown in Fig. 3, indicating the Ru_2 molecule is electrochemically active. Upon sweeping the potential between 0 V and 1.0 V (with respect to the AgQRE), a reduction-oxidation (redox) pair is observed after multiple cycles. The cathodic peak center is about 0.5 V, while the anodic peak center is about 0.39 V. When compared to the same Ru_2 molecule in solution,[32] this redox feature is consistent with the reversible oxidation of the diruthenium core going from Ru_2(III, II) to Ru_2(III, III). Therefore, the Ru_2 molecules are robustly integrated to the SiO_2/Si substrate and they are still electrochemically active, which is promising for solid state molecular memory.

In memory operations, an electrical bias should be applied to the gate electrode to induce the movement of charges between the semiconductor substrate and charge storage layer. The memory window performance of the Ru_2 devices and control samples is characterized by capacitance-voltage (C-V) hysteresis measurements at 1 MHz (see Fig. 4). The flatband voltage (V_{FB}) can be estimated from the C-V measurement. Its position is affected by the charge distribution in the capacitor structure. The hysteresis loop in C-V curves is due to the charge transfer between the Ru_2 SAM and Si substrate: electrons tunnel out of the molecules to Si at a sufficient negative V_G (oxidation) and tunnel back into the molecules at a sufficient positive V_G (reduction). Therefore, negative charges are stored in the molecules at positive gate voltage, causing C-V curves shifting toward the positive voltage direction, and positive charges are stored in the molecules at negative gate voltage, causing C-V curves shifting toward the negative voltage direction. In the result shown in Fig. 4(a), the Ru_2 molecular memory window can be defined as the shift of the flatband voltage ($\triangle V_{FB}$) from oxidation states to reduction states, which is about 5.2 V at an applied sweeping gate voltage of ±9 V at 1.0 MHz. The density of the trapped charges per unit area (N_t) can be roughly estimated from such C-V measurements by using the following formula:

$$N_t = C_{ox}\Delta V_{FB}/qA,$$

where C_{ox} represents the capacitance at the accumulation region, A is the effective device area, and q is the elementary charge. The density of the trapped charges in Ru_2 molecular memory devices at a sweeping voltage with ±9 V, 1 MHz is calculated as $7.3 \times 10^{12}\,cm^{-2}$, which means about 0.25 electron is stored in every Ru molecule in this condition. For comparison, the sample with the AUS linkage molecule but no Ru_2 molecules has a much smaller program $\triangle V_{FB}$ and almost no erase $\triangle V_{FB}$ [Fig. 4(b)] and the sample with no molecule showed even smaller $\triangle V_{FB}$ [Fig. 4(c)]. As shown in Fig. 4(d), the memory window, $\triangle V_{FB}$, of the no-molecule and AUS-only samples is much smaller than that of the Ru_2 molecular samples after the same voltage pulse, indicating the electron storage effect is primarily from the Ru_2 molecules.

Figure 5(a) shows the program/erase (P/E) speed characteristics of Ru_2 memory devices. Pulses of ±10 V with different widths were

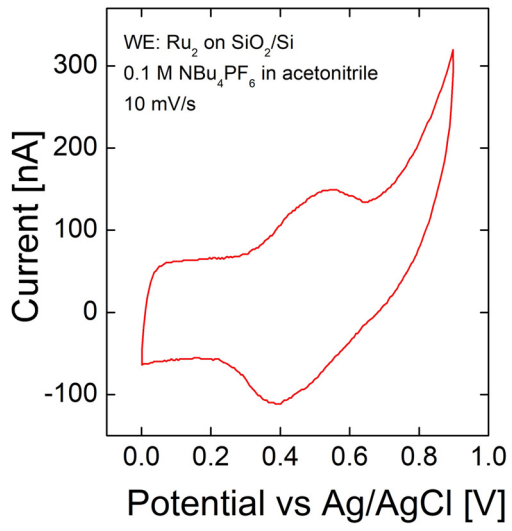

FIG. 3. Cyclic voltammetry scan of the Ru molecular system attached to SiOx/Si, as the working electrode, is shown. A redox couple due to the Ru-containing molecular layer is observed. The working electrolyte solution was 0.1 mol/l of tetrabutylammonium hexafluorophosphate in acetonitrile; the scan rate was 10 mV/s.

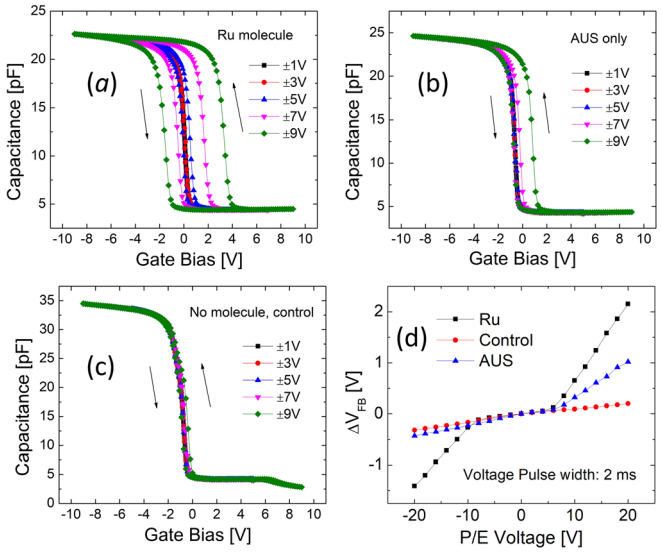

FIG. 4. High frequency (1 MHz) C-V measurements of memory devices, (a) with attached Ru-containing molecules, (b) with AUS linkage, and (c) with no molecules. (d) Summary of △VFB for these 3 structures as a function of P/E voltage with pulse width = 2 ms.

applied to determine the response speed of the P/E operations. Ru_2 molecule memory devices show a fast switch speed in both programing and erasing actions. Even with a pulse width as small as 10^{-5} s, the Ru_2 molecular memory devices still have a response and show $\triangle V_{FB}$ at 0.15 V (program) and 0.09 V (erase), respectively. We notice that the distribution of $\triangle V_{FB}$ during the erase operation is smaller compared to $\triangle V_{FB}$ for program operation under the same voltage amplitude. This asymmetry suggests that programming is faster than erasing in these Ru_2 molecular memory devices although the difference is not large. This difference in the program/erase response could be due to the difference in the density of traps for electrons and holes within the storage layer and the relative energetic positions of the molecular orbitals with respect to the band edges of the inorganic layers. Endurance characteristics of Ru_2 molecular memory devices are shown in Fig. 5(b). A P/E voltage of ±10 V with a 1 ms width at room temperature was applied to the top gate. The changes of V_{FB} after 10, 100, 1000, 10^4, and 10^5 P/E cycles are recorded. The degradation of $\triangle V_{FB}$ is only about 8% when compared with the initial value 0.45 V (programing $\triangle V_{FB}$) and 0.37 V (erasing $\triangle V_{FB}$) after 10^5 cycles. These data illustrate that this molecular memory device will not fail after even a large number of P/E cycles, indicating high reliability and stable switching endurance properties.

The loss of electrons from the charge storage layer over cycle-number or time typically means the likelihood of failure in information storage. Retention performance is one of the important standards to evaluate whether these memory devices are suitable for long-term data storage. The remaining charge stored in Ru_2 SAM can be estimated. As the final part of the memory device characterization, the retention property of Ru_2 molecular memory was investigated at room temperature by applying the gate voltage of ±10 V for 1 ms as shown in Fig. 5(c). It showed 0.05 V (program) and 0.04 V (erase) $\triangle V_{FB}$ shrinks after 10^4s compared to its initial value. By extrapolating the data with the tendency line in both the program state and erase state, the remnant memory window anticipated after 10 years is 72% of the initial V_{FB} shift, indicating that the charge loss from Ru_2 molecular SAM is acceptable for the nonvolatile application. The good retention property is mainly due to the AUS linkage molecule and good quality tunneling layer SiO_2.[31] The obtained retention property appears encouraging, considering that this Ru_2 molecular memory structure is only a prototype of the kinds of Ru molecules available with the molecular series. With a thorough engineering of each part and optimization of the ligands, great improvement can be anticipated. Retention characteristics can be related to many factors such as the nature of the tunneling barrier and the charge trap property. Both the intrinsic properties of Ru_2 molecules and the inserted AUS layer between the tunneling SiO_2 and the Ru_2 molecular SAM contribute to the charge retention. The AUS layer can be considered as a spatial insulator barrier, which helps preventing the charge from tunneling back to the Si. Its relative permittivity was estimated to be 3 from a previous report.[6] At the same time, the AUS layer likely creates an extra obstacle barrier for the charges switching between the Ru_2 molecules and the Si substrate, which is expected to slow the P/E process.

In summary, the Ru_2 molecular memory devices exhibit excellent nonvolatile behaviors. Compared to the previous works,[5–7] the MAROS capacitor structure exhibits a much larger memory window of 5.2 V, a relatively fast response for a 10^{-5} s P/E pulse, a longer retention time—estimated as >10 years, and negligible degradation after at least 10^5 P/E cycles.

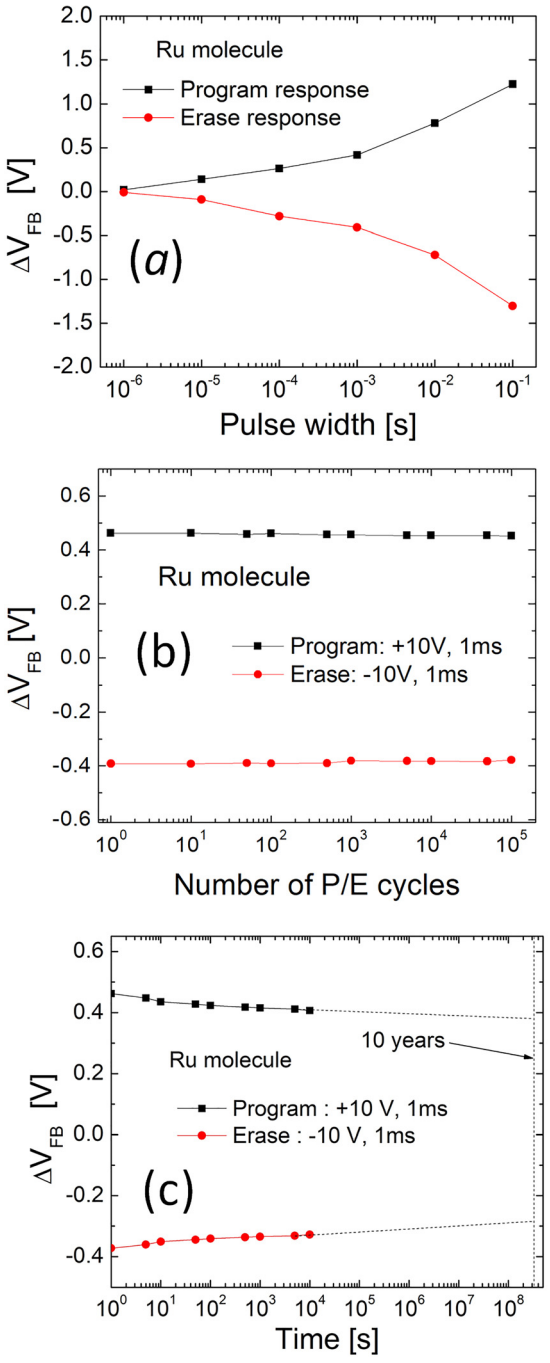

FIG. 5. (a) Response, (b) endurance, and (c) retention characteristics of Ru molecular memory devices. In (a), the P/E voltage is ±10 V. In (b), the flatband voltage is tested after P/E (±10 V, 1 ms) cycles. In (c), the gate voltage is ±10 V with 1 ms for P/E processes, respectively.

We have demonstrated a carefully designed method for fabricating high performance nonvolatile molecular memory with a new

redox-active diruthenium molecule. The characteristics of a molecular capacitor have been investigated. Due to the high surface coverage of charge-storage Ru_2 molecules on SiO_2, high-density charges can be stored in the Ru_2 molecular monolayer, leading to a large memory window as observed in high frequency C-V measurements. The programming/erasing response speeds and excellent endurance are also suitable for flashlike memory applications. In addition, the retention time performance is quite good due in part to the applied linkage AUS molecule. Overall, these Ru_2-based structures exhibit excellent performance as a prototype nonvolatile memory device, and these Ru_2 molecules are very attractive for next-generation memory applications.

The authors would like to acknowledge the support of NSF Grant Nos. ECCS-1809399 to Qiliang Li and CHE-1764347 to Tong Ren. Commercial equipment or materials are identified in this paper in order to specify the experimental procedure adequately. Such identification is not intended to imply recommendation or endorsement by NIST, nor is it intended to imply that the materials or equipment identified are necessarily the best available for the purpose.

REFERENCES

[1]F. Meng, Y.-M. Hervault, Q. Shao, B. Hu, L. Norel, S. Rigaut, and X. Chen, "Orthogonally modulated molecular transport junctions for resettable electronic logic gates," Nat. Commun. **5**, 3023 (2014).
[2]J. C. Scott and L. D. Bozano, "Nonvolatile memory elements based on organic materials," Adv. Mater. **19**(11), 1452–1463 (2007).
[3]M. Chhatwal, A. Kumar, S. K. Awasthi, M. Zharnikov, and R. D. Gupta, "An electroactive metallo–polypyrene film as a molecular scaffold for multi-state volatile memory devices," J. Phys. Chem. C **120**(4), 2335–2342 (2016).
[4]M. Chhatwal, A. Kumar, R. D. Gupta, and S. K. Awasthi, "A pyrene-based electropolymerized film as a solid-state platform for multi-bit memory storage and fluorescence sensing of nitroaromatics in aqueous solutions," J. Mater. Chem. C **4**(19), 4129–4133 (2016).
[5]A. Kumar, M. Chhatwal, D. A. Cristaldi, S. K. Awasthi, R. D. Gupta, and A. Gulino, "Chromogenic homo-dinuclear ruthenium(II) monolayer as a tunable molecular memory module for multibit information storage," J. Phys. Chem. C **119**(9), 5138–5145 (2015).
[6]S. Pookpanratana, H. Zhu, E. G. Bittle, S. N. Natoli, T. Ren, C. A. Richter, Q. Li, and C. A. Hacker, "Non-volatile memory devices with redox-active diruthenium molecular compound," J. Phys.: Condens. Matter **28**(9), 094009 (2016).
[7]C. Wu, W. Wang, and J. Song, "Molecular floating-gate organic nonvolatile memory with a fully solution processed core architecture," Appl. Phys. Lett. **109**(22), 223301 (2016).
[8]C.-W. Tseng, D.-C. Huang, and Y.-T. Tao, "Organic transistor memory with a charge storage molecular double-floating-gate monolayer," ACS Appl. Mater. Interfaces **7**(18), 9767–9775 (2015).
[9]D. Beckmeier and H. Baumgärtner, "Metal-oxide-semiconductor diodes containing C60 fullerenes for non-volatile memory applications," J. Appl. Phys. **113**(4), 044520 (2013).
[10]C.-W. Tseng and Y.-T. Tao, "Electric bistability in pentacene film-based transistor embedding gold nanoparticles," J. Am. Chem. Soc. **131**(34), 12441–12450 (2009).
[11]H.-C. Chang, C.-L. Liu, and W.-C. Chen, "Nonvolatile organic thin film transistor memory devices based on hybrid nanocomposites of semiconducting polymers: Gold nanoparticles," ACS Appl. Mater. Interfaces **5**(24), 13180–13187 (2013).
[12]C.-W. Tseng, D.-C. Huang, and Y.-T. Tao, "Azobenzene-functionalized gold nanoparticles as hybrid double-floating-gate in pentacene thin-film transistors/memories with enhanced response, retention, and memory windows," ACS Appl. Mater. Interfaces **5**(19), 9528–9536 (2013).
[13]S.-T. Han, Y. Zhou, Q. D. Yang, L. Zhou, L.-B. Huang, Y. Yan, C.-S. Lee, and V. A. L. Roy, "Energy-band engineering for tunable memory characteristics through controlled doping of reduced graphene oxide," ACS Nano **8**(2), 1923–1931 (2014).
[14]J. Xiang, T.-K. Wang, Q. Zhao, W. Huang, C.-L. Ho, and W.-Y. Wong, "Ferrocene-containing poly(fluorenylethynylene)s for nonvolatile resistive memory devices," J. Mater. Chem. C **4**(5), 921–928 (2016).
[15]W. Lv, H. Wang, L. Jia, X. Tang, C. Lin, L. Yuwen, L. Wang, W. Huang, and R. Chen, "Tunable nonvolatile memory behaviors of PCBM–MoS_2 2D nanocomposites through Surface deposition ratio control," ACS Appl. Mater. Interfaces **10**(7), 6552–6559 (2018).
[16]G. Ligorio, M. V. Nardi, and N. Koch, "Lithography-free miniaturization of resistive nonvolatile memory devices to the 100 nm Scale by glancing angle deposition," Nano Lett. **17**(2), 1149–1153 (2017).
[17]H.-Y. Chi, H.-W. Hsu, S.-H. Tung, and C.-L. Liu, "Nonvolatile organic field-effect transistors memory devices using supramolecular block copolymer/functional small molecule nanocomposite electret," ACS Appl. Mater. Interfaces **7**(10), 5663–5673 (2015).
[18]A.-D. Yu, T. Kurosawa, M. Ueda, and W.-C. Chen, "Polycyclic arene-based D–A polyimide electrets for high-performance n-type organic field effect transistor memory devices," J. Polym. Sci. Part A **52**(1), 139–147 (2014).
[19]S.-W. Cheng, T. Han, T.-Y. Huang, Y.-H. C. Chien, C.-L. Liu, B. Z. Tang, and G.-S. Liou, "Novel organic phototransistor-based nonvolatile memory integrated with UV-sensing/green-emissive aggregation enhanced emission (AEE)-active aromatic polyamide electret layer," ACS Appl. Mater. Interfaces **10**(21), 18281–18288 (2018).
[20]L. Song, Y. Wang, Q. Gao, Y. Guo, Q. Wang, J. Qian, S. Jiang, B. Wu, X. Wang, Y. Shi, Y. Zheng, and Y. Li, "Speed up ferroelectric organic transistor memories by using two-dimensional molecular crystalline semiconductors," ACS Appl. Mater. Interfaces **9**(21), 18127–18133 (2017).
[21]W. Y. Kim, H.-D. Kim, T.-T. Kim, H.-S. Park, K. Lee, H. J. Choi, S. H. Lee, J. Son, N. Park, and B. Min, "Graphene–ferroelectric metadevices for nonvolatile memory and reconfigurable logic-gate operations," Nat. Commun. **7**, 10429 (2016).
[22]H. Zhu and Q. Li, "Novel molecular non-volatile memory: Application of redox-active molecules," Appl. Sci. **6**(1), 7 (2016).
[23]C. Li, W. Fan, B. Lei, D. Zhang, S. Han, T. Tang, X. Liu, Z. Liu, S. Asano, M. Meyyappan, J. Han, and C. Zhou, "Multilevel memory based on molecular devices," Appl. Phys. Lett. **84**(11), 1949–1951 (2004).
[24]H. Zhu, C. A. Hacker, S. J. Pookpanratana, C. A. Richter, H. Yuan, H. Li, O. Kirillov, D. E. Ioannou, and Q. Li, "Non-volatile memory with self-assembled ferrocene charge trapping layer," Appl. Phys. Lett. **103**(5), 053102 (2013).
[25]H. Zhu, S. J. Pookpanratana, J. E. Bonevich, S. N. Natoli, C. A. Hacker, T. Ren, J. S. Suehle, C. A. Richter, and Q. Li, "Redox-active molecular nanowire flash memory for high-endurance and high-density nonvolatile memory applications," ACS Appl. Mater. Interfaces **7**(49), 27306–27313 (2015).
[26]J. R. Heath, "Molecular electronics," Annu. Rev. Mater. Res. **39**(1), 1–23 (2009).
[27]R. J. Hamers, S. K. Coulter, M. D. Ellison, J. S. Hovis, D. F. Padowitz, M. P. Schwartz, C. M. Greenlief, and J. N. Russell, "Cycloaddition chemistry of organic molecules with semiconductor surfaces," Acc. Chem. Res. **33**(9), 617–624 (2000).
[28]W.-Y. Lee, H.-C. Wu, C. Lu, B. D. Naab, W.-C. Chen, and Z. Bao, "n-Type doped conjugated polymer for nonvolatile memory," Adv. Mater. **29**(16), 1605166 (2017).
[29]Y. Zhou, S.-T. Han, Y. Yan, L. Zhou, L.-B. Huang, J. Zhuang, P. Sonar, and V. A. L. Roy, "Ultra-flexible nonvolatile memory based on donor-acceptor diketopyrrolopyrrole polymer blends," Sci. Rep. **5**, 10683 (2015).
[30]W.-Z. Chen and T. Ren, "Preparation and characterization of a family of Ru_2 compounds bearing iodo/ethynyl substituents on the periphery," Inorg. Chem. **45**(20), 8156 (2006).
[31]S. Pookpanratana, I. Savchenko, S. N. Natoli, S. P. Cummings, L. J. Richter, J. W. F. Robertson, C. A. Richter, T. Ren, and C. A. Hacker, "Attachment of a diruthenium compound to Au and SiO_2/Si surfaces by "click" chemistry," Langmuir **30**(34), 10280–10289 (2014).
[32]W. P. Forrest, Z. Cao, W.-Z. Chen, K. M. Hassell, A. Kharlamova, G. Jakstonyte, and T. Ren, "Decorating diruthenium compounds with Fréchet dendrons via the click reaction," Inorg. Chem. **50**(19), 9345–9353 (2011).